ELSEVIER

Polymer 42 (2001) 1023–1033

polymer

www.elsevier.nl/locate/polymer

Infrared spectroscopic analysis of poly(trimethylene terephthalate)

K.J. Kim[a,*], J.H. Bae[a], Y.H. Kim[b]

[a]*Department of Polymer and Fiber Materials Technology, College of Environment and Applied Chemistry, Kyung Hee University, Kyunggi-do 449-701, South Korea*

[b]*Department of Textile Engineering, Soong Sil University, Seoul 156-743, South Korea*

Received 1 February 2000; received in revised form 25 April 2000; accepted 9 June 2000

Abstract

With factor analysis of IR spectra obtained from undrawn poly(trimethylene terephthalate) (3GT) films annealed under various conditions, pure crystalline and amorphous spectra can be extracted and absorption peaks of each pure spectrum can be characterized. A fraction of crystalline phase in an annealed sample was obtained by curve-fitting the sample spectrum with two pure spectra on the basis of the least-squares method. The fraction of the crystalline phase obtained from this method showed a very good correlation to the crystallinity obtained by density measurement. Polarization characteristics of 3GT absorption peaks were determined from on-line measurement of polarized IR spectra of 3GT film under extension. Intrinsic transition moment angles of asymmetric and symmetric stretching vibrations of CH_2, several CH_2 rocking bands, and the 1037 cm^{-1} band were obtained experimentally in conjunction with changes in the dichroic ratio of C=O stretching vibration of the 3GT molecular chain as a function of draw ratio. The analysis of changes in the IR spectrum of 3GT under cyclic loading and unloading revealed no crystal–crystal transitions, such as reversible $\alpha \rightarrow \beta$ transition of the poly(butylene terephthalate).

Keywords: Poly(trimethylene terephthalate); Crystalline and amorphous phases; Intrinsic transition moment angle and dichroic ratio

1. Introduction

Poly(ethylene terephthalate) (2GT) and poly(butylene terephthalate) (4GT) of poly(*m*-methylene terephthalate) polymers have been produced commercially for more than 50 years. Poly(trimethylene terephthalate) (3GT) was first patented in 1941, but it was not until the 1990s, when Shell Chemicals developed a low-cost method of producing 1,3-propandiol, the starting raw material for 3GT, that the commercial production of 3GT became a reality. Therefore there have not been so many systematic research reports on the intrinsic physicochemical properties of 3GT as compared with studies on 2GT and 4GT. The physical properties of 3GT are known to be much different from those of the better known even-numbered homologues, 2GT and 4GT. [1,2] Fibers made from 3GT provide resilience and elastic recovery better than 2GT and 4GT and equal to or even better than nylon 6 and nylon 66. Owing to the particularly high elasticity and recovery, the 3GT fibers may be used widely in garments requiring good resilience and substituted for nylons in carpets and other floor coverings. As these big differences in physical properties are associated with differences in the chain conformation and segmental chain orientation in a uniaxially drawn state, we focused our attention on the understanding of the changes in the chain conformation and chain orientation during annealing and stretching using infrared spectroscopy and the obtaining of the transition moment angles of several important vibrational bands not reported to date.

2. Experimental

Isotropic amorphous 3GT film (intrinsic viscosity 0.85 dl/g, in 1,1,2,2-tetrachloroethane/phenol (1:1 w/w) solution at 20°C) was prepared by melt-pressing and subsequently quenching in ice water. Its glass transition temperature, cold crystallization temperature, and melting temperature were 41, 68, and 228°C, respectively. Subsequently, isotropic amorphous 3GT films were annealed at the temperature range of 70–180°C for different lengths of time(3–24 h) to obtain samples having various degrees of crystallinity. Density data were obtained using a density gradient column consisting of carbon tetrachloride and *n*-heptane at 25°C.

* Corresponding author. Tel.: +82-331-201-2518; fax: +82-331-202-9484.

E-mail address: kjkim@khu.ac.kr (K.J. Kim).

0032-3861/01/$ - see front matter © 2000 Published by Elsevier Science Ltd.
PII: S0032-3861(00)00424-9

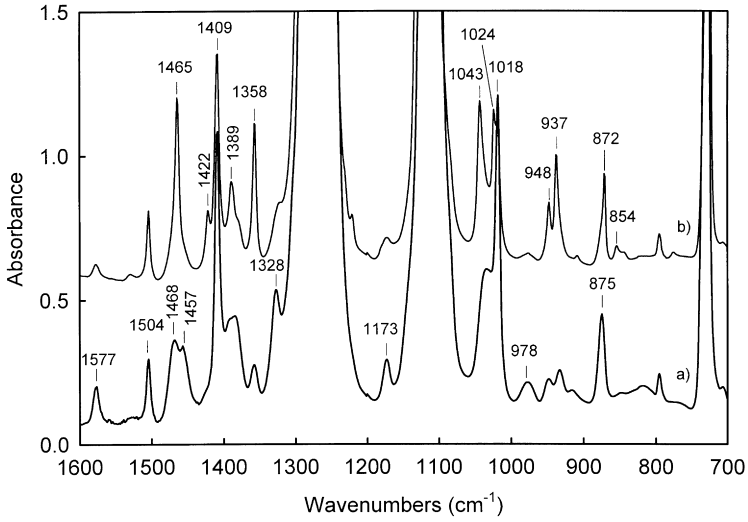

Fig. 1. The absorbance IR spectra of the melt-quenched and annealed 3GT samples. (a) Melt-quenched; (b) annealed at 200°C for 24 h.

The IR measurements were carried out using a Brüker IFS-66V FT-IR spectrometer with a resolution of 2 cm^{-1} and a scan number of 32. The in situ polarized FT-IR spectra parallel and perpendicular to MD (machine direction) and load–elongation curves were recorded during drawing at 35°C. In order to study the elastic recovering properties and crystalline transition of 3GT, we measured the in situ polarized FT-IR spectra and cyclic load–extension curves simultaneously during the oscillation of the four-times drawn sample at 2 mm/min at room temperature using a specially designed extensometer equipped with an automatic polarizer rotator and a load cell. Maximum extension ranges were varied from 5 to 20%.

Table 1
Factor analysis of FT-IR spectra of 3GT annealed under various conditions in the region of 1600 to 750 cm^{-1} (the regions of 1305–1220 and 1135–1080 cm^{-1} were excluded in the calculation of factor analysis due to deviation from Beer's law)

Component, k	Annealing conditions	Eigenvalue	IND × 10^4
1	70°C, 3 h	14.7662	0.2046
2	70°C, 6 h	0.0927	0.1854
3	70°C, 12 h	0.0523	0.1913
4	100°C, 12 h	0.0229	0.1985
5	100°C, 24 h	0.0207	0.2087
6	120°C, 6 h	0.0138	0.2264
7	120°C, 12 h	0.0109	0.2455
8	120°C, 24 h	0.0063	0.2857
9	150°C, 3 h	0.0044	0.3495
10	150°C, 12 h	0.0034	0.4449
11	150°C, 24 h	0.0024	0.6127
12	180°C, 6 h	0.0019	0.8913
13	180°C, 24 h	0.0012	1.5644
14	200°C, 12 h	0.0005	5.3384
15	200°C, 24 h	0.0003	–

3. Results and discussion

3.1. Crystalline and amorphous phases

The IR spectra of 3GT in the amorphous state and after annealing at 200°C for 24 h are shown in Fig. 1. Large increases in the absorbance of the 1465, 1358, 1043, 1024, 948, and 937 cm^{-1} bands are observed while decreases in the 1577, 1328, 1173, 1018, and 978 cm^{-1} bands, and the new advent of 1422 and 854 cm^{-1} bands after annealing are observed. On the other hand, there is no significant change in intensity at 1504 cm^{-1} after annealing. When the IR absorbance spectrum is normalized for quantitative analysis, this band can be used as an internal thickness standard band as in the IR spectra of 2GT and 4GT [3,4]. Since annealing is known to produce a significant increase in the degree of crystallinity, the bands showing increases and decreases in absorbance can be identified as crystalline and amorphous characteristics, respectively. More sophisticated identification of crystalline and amorphous bands is possible only when pure amorphous and crystalline spectra can be extracted. Considering that, most of the characteristic bands overlap with each other, the extraction of each pure component spectrum by using only the mutual subtraction between the spectra of the two samples having different degrees of crystallinity, is not possible. In this case, the factor analysis (FA) technique is the sole method to extract each pure amorphous and crystalline spectrum from a series of spectra of the samples with various degrees of crystallinity. The basic concepts of FA and further details are explained well elsewhere [5–12].

For FA, a series of samples having different degrees of crystallinity were prepared by annealing melt-quenched films at temperatures ranging from 70 to 200°C for 3–25 h. The number of samples (N_s) was 15. A frequency

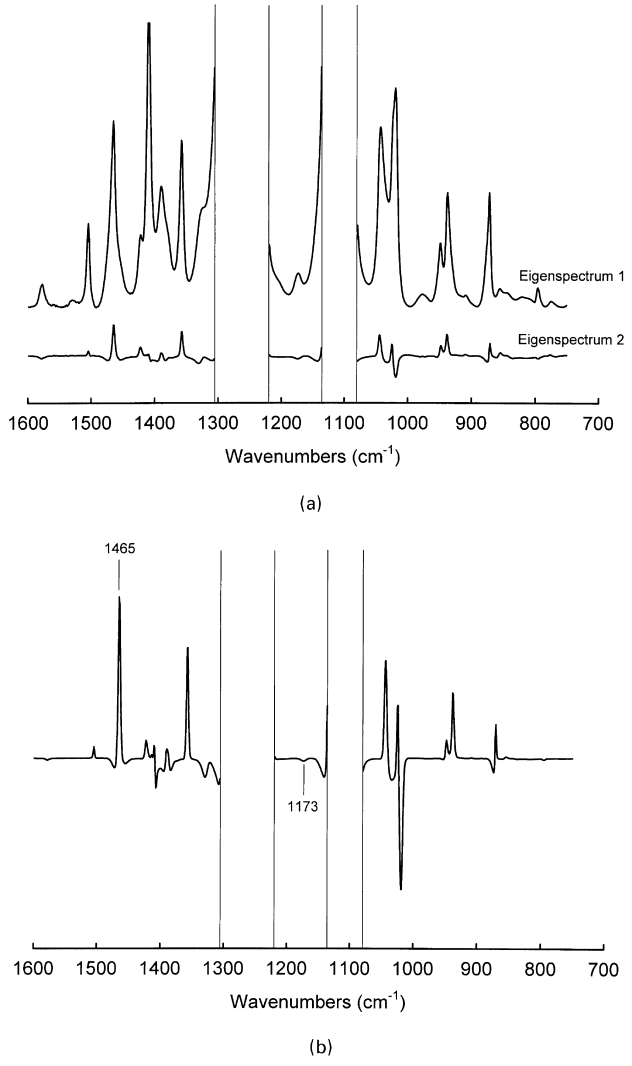

Fig. 2. (a) Abstract eigenspectra for the annealed 3GT system. (b). Cross product spectrum of the first two abstract eigenspectra.

range of 1600–750 cm^{-1} was used in the analysis. All the raw spectra were corrected with an appropriate baseline. The absorbance data in the range of 1305–1220 and 1135–1080 cm^{-1} were excluded in FA, because most of absorbance data in these two regions exceeded the maximum absorbance, above which Beer's law is no longer satisfied. The absorbance was normalized by dividing the baseline-corrected spectrum by the square root of the sum of the squared absorbances in the newly set ranges. The resultant data matrix $\mathbf{A}$ is composed of N_s column matrices, each of which has N_w normalized absorbance data points in the frequency space. From Beer's law, the matrix $\mathbf{A}$ of dimensions $N_w \times N_s$ can be written as $\mathbf{A} = \mathbf{PC}$, where $\mathbf{P}$ is the pure component spectrum matrix of dimensions $N_w \times N_c$, N_c is the number of pure components, and $\mathbf{C}$ is a concentration matrix of dimensions $N_s \times N_s$. Now the covariance matrix $\mathbf{Q}$ of dimensions $N_s \times N_s$ is obtained from $\mathbf{Q} = \mathbf{A}^T\mathbf{A}$, where $\mathbf{A}^T$ is the transpose of $\mathbf{A}$. The eigenvalue matrix $\boldsymbol{\Lambda}$ and the eigenvector matrix $\mathbf{S}$ of dimensions $N_s \times N_s$ are therefore obtained by $\mathbf{S}^{-1}\mathbf{QS} = \boldsymbol{\Lambda}$.

The results of FA are summarized in Table 1. The value of N_c is equal to the number of nonzero eigenvalues. Since an error is always included in every measurement, it is not easy to determine the number of nonzero eigenvalues. In this case Malinowski's factor indicator function (IND) is used as a good criterion to estimate the magnitude of error included in each eigenvalue. The IND is known to reach a minimum, when the correct number of nonzero eigenvalues is employed [13–15]. The IND reached a minimum at $k = 2$, indicating that the two factors, such as amorphous and crystalline components, were present. The magnitude of the eigenvalues (λ_k's) is a measure of the relative importance of corresponding eigenvectors. Therefore two abstract eigenspectra ($\mathbf{U}_1$ and $\mathbf{U}_2$) can be constructed by using the first two eigenvectors ($\mathbf{S}_1$ and $\mathbf{S}_2$) and the real data matrix $\mathbf{A}$ from the relation

$$(\mathbf{U}_1\mathbf{U}_2) = (\mathbf{A}_1\mathbf{A}_2\cdots\mathbf{A}_{N_s})(\mathbf{S}_1\mathbf{S}_2).$$

The two abstract eigenspectra are shown in Fig. 2a. From the cross product of the eigenspectra, it can be seen that the negative peak group and positive peak group represent amorphous and crystalline characteristics, respectively (Fig. 2b). The most intense 1465 cm^{-1} peak of all the positive peaks was chosen as the crystalline reference peak. On the other hand, instead of choosing the most intense 1019 cm^{-1} peak of negative peaks as an amorphous reference peak, the relatively weak negative peak at 1173 cm^{-1} was chosen, because it does not overlap with any of the crystalline bands. The pure crystalline spectrum could be isolated by subtracting the $\mathbf{U}_2$ spectrum from the $\mathbf{U}_1$ spectrum until the 1173 cm^{-1} peak was no longer visible. Similarly, the pure amorphous spectrum was obtained by subtracting the $\mathbf{U}_2$ spectrum from the $\mathbf{U}_1$ spectrum until the 1465 cm^{-1} peak was not observed. The end point of each subtraction procedure was based on the exponential minimization criterion suggested by Kim and Bae [16]. And finally, the crystalline reference spectrum $\mathbf{P}_1$ and the amorphous reference spectrum $\mathbf{P}_2$ were obtained by normalizing the isolated pure spectra using the same method applied to the normalization of raw data matrix $\mathbf{A}$.

For the ethylene glycol unit (O–CH_2–CH_2–O) of 2GT there are a large range of conformational possibilities, e.g. *ttt*, *tgt*, *ggg*, *tgg*, and *gtg*. Only an all-*trans* conformation is possible in the crystalline phase, while the populations for the amorphous phase are estimated as 63% *tgt*, 26% *tgg*, and 7% *ttt* with the other conformations (*ggg* and *gtg*) being present in very low quantities [17]. For the trimethylene glycol unit (O–CH_2–CH_2–CH_2–O) of 3GT, the situation is quite different. The crystalline structure of 3GT is *tggt*, whose conformational energy is lowest. Since the next highest-energy conformation is *gttg* and the all-*trans tttt* conformation is the highest-energy state possibility, the *gttg* conformation is most populous in the amorphous phase of 3GT [18]. Thus the annealing of 3GT results in both the

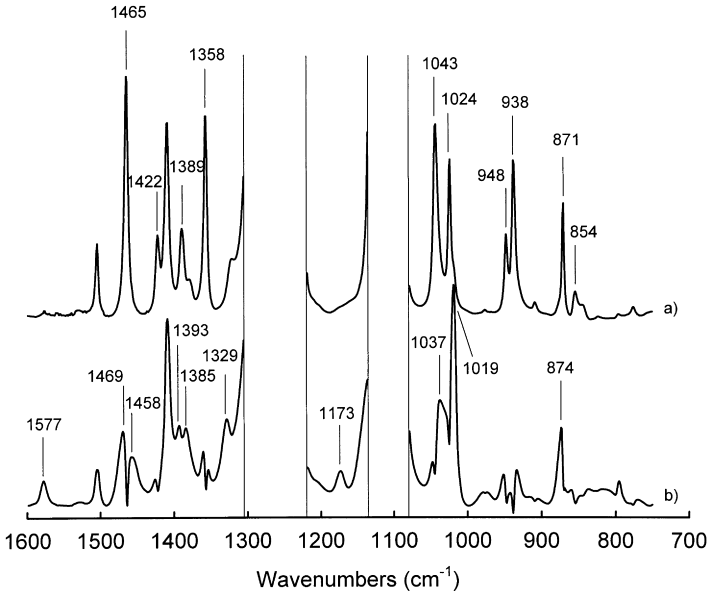

Fig. 3. Extracted pure-component spectra from the annealed 3GT system. (a) Pure crystalline phase; (b) pure amorphous phase.

trans-to-*gauche* conversion for the inner two C–C bonds and *gauche*-to-*trans* conversion for the outer two C–O bonds. Additionally, the population ratios of the conformations in the amorphous phase are changed [19]. The two pure component spectra are shown in Fig. 3. The crystalline bands are narrow and well defined. The breadth of the amorphous-phase bands reflects a somewhat wide distribution of conformations present.

In the pure crystalline spectrum one finds bands at 1465, 1422, 1389, 1358, 1043, 1024, 948, 938, 871, and 854 cm^{-1}. The 1465 cm^{-1} band is associated with the scissoring mode of CH_2 in the crystalline phase. The 1358 cm^{-1} band, the 1043 cm^{-1} band, and the 1024 cm^{-1} band are assigned to the B_u CH_2 wagging mode in the crystalline phase, the A_g C–C stretching mode of a *gauche* conformer in the crystalline phase, and the B_{2u} CH in-plane bending of the phenylene ring in the crystalline phase, respectively. The 948 and 938 cm^{-1} bands are assigned to the CH_2 rocking mode of the crystal and the 871 cm^{-1} band is associated with the B_{3u} CH out-of-plane bending of phenylene ring and/or B_u C–O–C deformation in the crystalline phase [20]. However, the 1422 and 854 cm^{-1} bands are not identified as yet. The 1504 and 1409 cm^{-1} bands in the pure crystalline spectrum are also seen in the pure amorphous one. These two bands are assigned to the B_{1u} C–C and the B_{2u} C–C stretching modes, respectively. In the pure amorphous spectrum bands are seen at 1577, 1469, 1458, 1393, 1385, 1329, 1173, 1037, 1019, and 874 cm^{-1}. The 1469 and 1458 cm^{-1} bands are assigned to the CH_2 bending in the amorphous phase, and the 1173 cm^{-1} band is assigned to the A_g CH in-plane bending of phenylene ring in the amorphous phase. The 1037 cm^{-1} band, the 1019 cm^{-1} band, and the 874 cm^{-1} band are assigned to the A_g C–C stretching mode of a *gauche* conformer in the amorphous phase, the B_{2u} CH in-plane bending of phenylene ring in the amorphous phase, and the B_{3u} CH in-plane bending of phenylene ring and/or B_u C–O–C deformation in the amorphous phase, respectively.

Since the two pure component spectra $\mathbf{P}_1$ and $\mathbf{P}_2$ are extracted from FA, one can evaluate the degree of crystallinity for the annealed 3GT sample by using the non-weighted least-squares curve-fitting (LS) method suggested by Haaland and Eastering [21]. Since $\mathbf{A} = \mathbf{PC}$ from Beer's law, $\mathbf{C}$ matrix representing the degree of crystallinity can be obtained from the relation $\mathbf{C} = (\mathbf{P}^T\mathbf{P})^{-1}\mathbf{P}^T\mathbf{A}$ derived through $\mathbf{P}^T\mathbf{A} = \mathbf{P}^T\mathbf{PC}$. More details about LS method are not mentioned here. In order to examine the validity of the degree of crystallinity by LS in conjunction with FA, we plotted the FA-crystallinity versus the density-crystallinity obtained from the measurement of the density of the annealed sample in Fig. 4. As shown in Fig. 4, one can observe a good linear correlation between the two. This good correlation seems to result from the fact that the semi-crystalline structure of 3GT can be analyzed by the linear combination of the fraction of each crystalline and amorphous phase based on the so-called two-phase model. Now evaluation of the crystallinity by FA in conjunction with LS is possible without the tedious and time-consuming density measurement any longer.

3.2. Infrared dichroism of 3GT upon uniaxial stretching

Fig. 5 shows the polarized IR spectra of 3GT after 300% extension. One can distinguish the σ-band from π-band. The typical σ-bands are at 2967 (asymmetric stretching of CH_2), 2901 (symmetric stretching of CH_2), 1720 (stretching of C=O), 1468 (CH_2 scissoring), 948 (CH_2 rocking), 874 (CH out-of-plane bending of phenylene ring and/or C–O–C deformation), and 729 cm^{-1} (CH in-plane and/or out-of

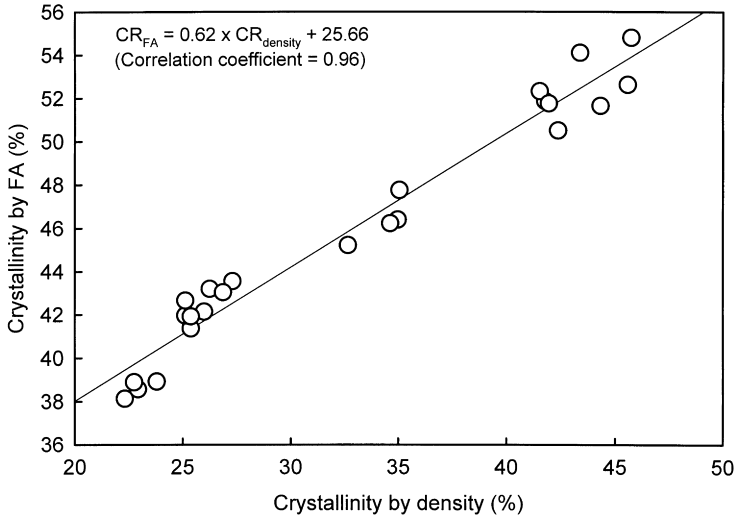

Fig. 4. Correlation of crystallinity as determined by density and crystallinity determined by FA.

plane bending of phenylene ring) and whereas the typical π-bands are at 1357 (CH_2 wagging), 1037 (A_g C–C stretching mode of a *gauche* conformer), 1018(CH in-plane bending of phenylene ring), and 935 cm^{-1} (CH_2 rocking). Some crystalline peaks at 1357, 948, and 937 cm^{-1} show a very weak intensity in the polarized spectra after 300% extension, whereas the other crystalline peaks at 1422, 1043, and 854 cm^{-1} do not appear. These results indicate that the drawing of 3GT at 38°C does not induce crystallization as much as annealing.

The dichroic ratio (D_0) of an ideally oriented polymer with perfect alignment of its molecules parallel to the fiber axis is expressed as

$$D_0 = 2\cot^2 \alpha_v \tag{1}$$

where α_v is transition moment angle of vibration.

The observed dichroic ratio of a non-ideally oriented polymer D is given in terms of D_0 and Hermans' orientation function f [22–25].

$$D = \frac{1 + (1/3)(D_0 - 1)(1 + 2f)}{1 + (1/3)(D_0 - 1)(1 - f)} \tag{2}$$

which is reduced to

$$f = \frac{(D - 1)(D_0 + 2)}{(D + 2)(D_0 - 1)} \tag{3}$$

Thus, if D_0 (or α_v) is known, the degree of chain orientation f of a uniaxially drawn polymer is then calculated from the measured dichroic ratio D using Eq. (3). D_0 can be determined from a theoretical molecule model or estimated from the measured value of D and the value of f obtained from other methods such as X-ray diffraction, sonic velocity, or birefringence by using Eq. (3). The value of D_0 for each vibrational band of 3GT is not known to date. The determination of new intrinsic D_0 values for each vibration of 3GT would enable us to evaluate the degree of chain orientation by only simple IR measurement without further complicated and time-consuming measurements.

Because of associations with isolated stretching vibration modes without coupling with other vibrations and due to the absence of differences in peak position and extinction coefficient between the crystalline and amorphous regions, CH_2 asymmetric stretching (2967 cm^{-1}) and symmetric stretching (2901 cm^{-1}) bands are very useful in evaluating the average orientation function of the sample. The C=O stretching vibration band (1720 cm^{-1}) can also be another good candidate for the evaluation of chain orientation, because the C=O stretching vibration has no coupling

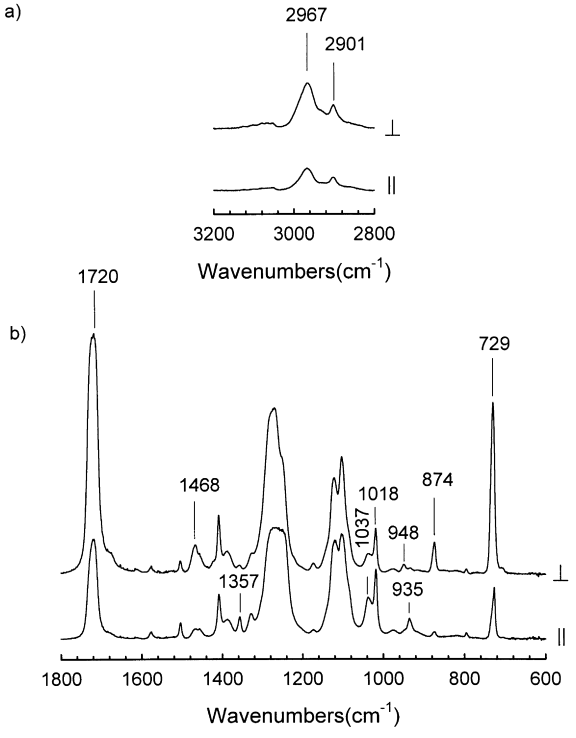

Fig. 5. Polarized IR spectra of the 3GT sample at 300% elongation.

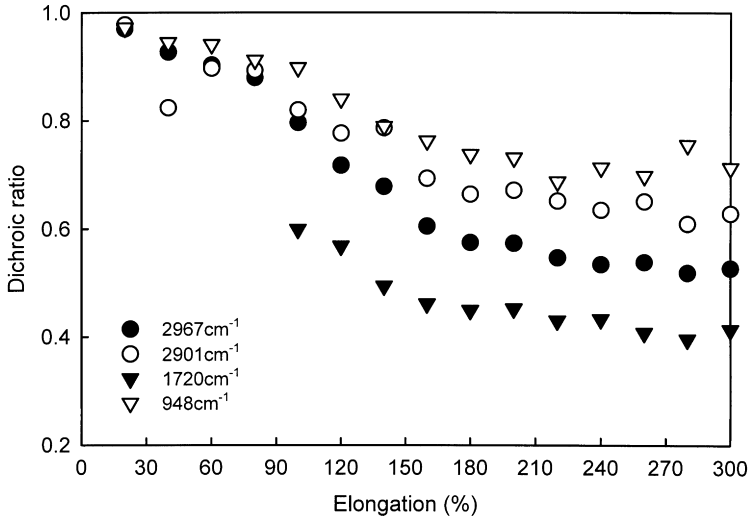

Fig. 6. The variation of the dichroic ratios of the σ-bands upon uniaxial stretching.

with any other vibration mode and thus the angle between the displacement vector of the C=O of the carbonyl group and the main chain of 3GT is exactly same as the angle between the transition moment angle of the C=O vibration and the main chain.

Since the CH_2 and C=O stretching vibrations are both σ characteristic, we must assume that the transition moments of the CH_2 and C=O stretching vibrations are oriented randomly in the plane perpendicular to the draw direction when these two characteristic bands are used to obtain changes in the average orientation function of molecular chain during uniaxial drawing. If the transition moment has a preferred orientation to the film surface, changes in the dichroic ratios of stretching vibrations of CH_2 and C=O depend not only on the degree of the orientation of the molecular chain by drawing, but also on the degrees of the orientation of CH_2 and C=O to the film surface. In this study, we used C=O stretching vibration data in evaluating the degree of chain orientation, since it is much easier to calculate $\alpha_{C=O}$ from the crystal lattice parameters of 3GT and the fractional coordinates of each atom in the unit cell are known from X-ray diffraction measurements [26]. Fractional coordinates of the atoms C and O of the carbonyl group can be transformed into Cartesian coordinates, from which the displacement vector coordinates of C=O can be calculated. Therefore, the angle $\alpha_{C=O}$ between this displacement vector and molecular chain axis (unit vector of *c*-axis) was obtained and finally $D_{0,C=O}$ was obtained from Eq. (1). Since 3GT has two monomeric units in a crystal unit lattice, four different C=O carbonyl groups must be considered in calculating the average value of $\cot^2 \alpha_{C=O}$. However, considering a center of symmetry, only one pair of carbonyl groups can be involved [26]. In this way, the average value of $\cot^2 \alpha_{C=O}$ was calculated to be 0.0738 and $D_{0,C=O}$ was 0.1476 from Eq. (1).

Although the same calculation can be applied to the CH_2 stretching vibrations, the number of fractional coordinate sets considered are much more than for the C=O stretching vibration. Thus, we did not use the CH_2 vibration data in obtaining the degree of chain orientation.

Changes in dichroic ratios of several σ-bands are depicted in Fig. 6. The dichroic ratios decrease rapidly from 80 to 170% of elongation, but after that there are no great reductions in slope. The dichroic ratio of C=O in the early elongation stage could not be obtained exactly, since the absorbance exceeded 2 due to the high polarizability of C=O and the sample thickness. With the intrinsic $D_{0,C=O}$ value and measured dichroic ratio $D_{C=O}$, the degree of chain orientation was obtained as a function of elongation using Eq. (3). The results are shown in Fig. 7. The increase in orientation is very slow after 160% of elongation, and the maximum orientation is about 0.62.

The transition moment angle of the 3GT CH_2 stretching vibration can be obtained by using the average orientation of the molecular chain calculated from the dichroic ratio of C=O stretching. This calculation needs one more assumption that the conformation and the fractional coordinates of atoms in the lattice does not change upon drawing, i.e. there are no changes in every transition moment angle upon drawing. Fig. 8 shows the plot of the average degree of chain orientation calculated from dichroic ratio of symmetric stretching of C=O versus $-(D-1)/(D+2)$ for the asymmetric stretching vibration band of CH_2 (2967 cm^{-1}). According to Eq. (3), this plot should be linear through the origin, because the slope is to be $-(D_0+2)/(D_0-1)$. Thus, from the slope, D_{0,ν_{as},CH_2} and the transition moment angle α_{ν_{as},CH_2} the asymmetric vibration band of CH_2 were calculated to be 0.3286 and 67.93°, respectively. Using these results and the dichroic ratio data of the CH_2 asymmetric vibration shown in Fig. 6, the changes in average molecular orientation function of 3GT could be obtained through the entire range of elongation as shown in Fig. 9a. The degree of orientation increases slowly up to 80% elongation, and then it increases rapidly up to 180% elongation.

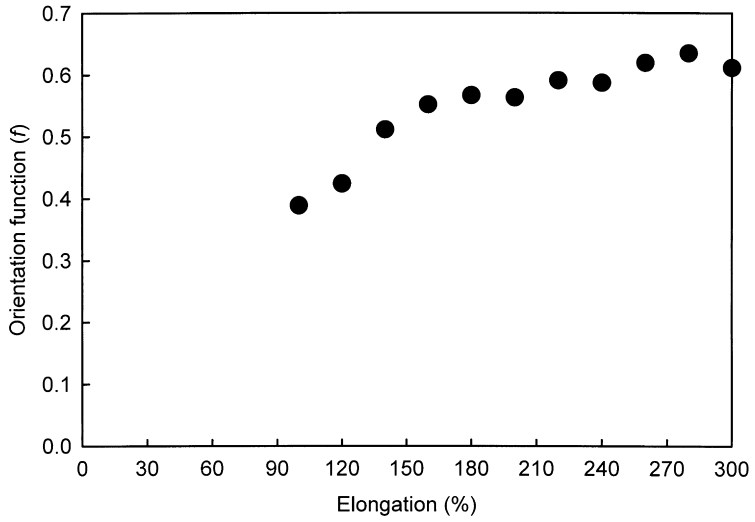

Fig. 7. The variation of the orientation function based on the peak at 1720 cm^{-1} upon uniaxial stretching.

Thereafter the increase in the degree of chain orientation decreases. Fig. 9b shows the load–elongation curve of 3GT during the measurement of in situ polarized IR spectra as a function of drawing. The trend of increase in load upon drawing is nearly same as that of the increase in the degree of chain orientation up to 180% elongation. Thereafter the trends do not coincide. The load still linearly increases up to the breaking point without the necking phenomenon that is observed generally in the drawing process of the thermoplastic polymer, whereas the chain orientation is not increased as much as load. To our knowledge, we cannot explain why the load can be linearly increased while the increasing rate of the chain orientation is reduced.

Similarly, from the average degree of chain orientation through the entire range of elongation, the transition moment angles of other σ characteristic bands such as the symmetric stretching vibration of CH_2 (2901 cm^{-1}) and rocking band of CH_2 (948 cm^{-1}) could be obtained (ca. $D_{0,\nu_s,CH_2} = 0.4569$, $\alpha_{\nu_s,CH_2} = 64.45°$ and $D_{0,\rho CH_2} = 0.5691$, $\alpha_{\rho CH_2} = 61.92°$). Their results are shown in Fig. 10. Both peaks show a good linear correlation throughout the entire range.

Changes in the dichroic ratios of several π characteristic bands at 1357 cm^{-1} (CH_2 wagging), 1037 cm^{-1} (C–C symmetric stretching of glycol unit), and 935 cm^{-1} (CH_2 rocking) are shown in Fig. 11. There are very slight changes in early stage of drawing, but rapid increases in dichroic ratio are observed from 90 to 180% of elongation. The intrinsic dichroic ratio D_0 and transition moment angle α_ν of π-bands could also be obtained from the linear plot of the average orientation function versus $(D-1)/(D+2)$. The transition moment angles of 1357, 1037, and 935 cm^{-1} bands were calculated to be 38.97, 42.38, and 32.41°,

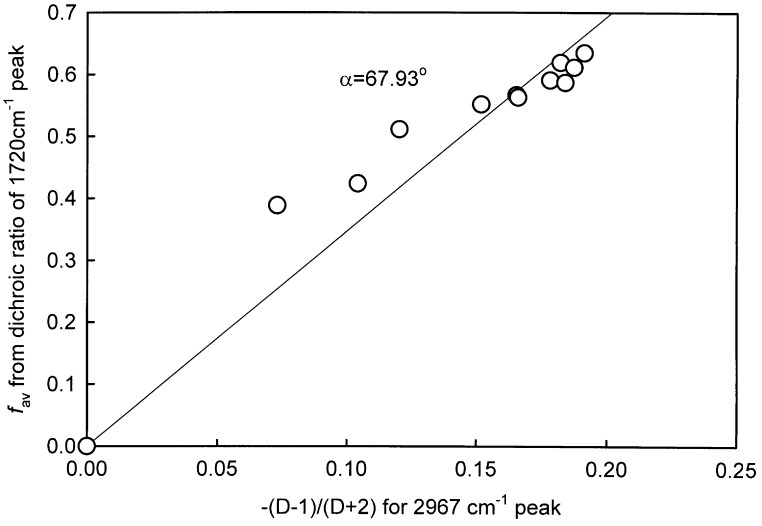

Fig. 8. Determination of the transition moment angle α_ν for the 2967 cm^{-1} band.

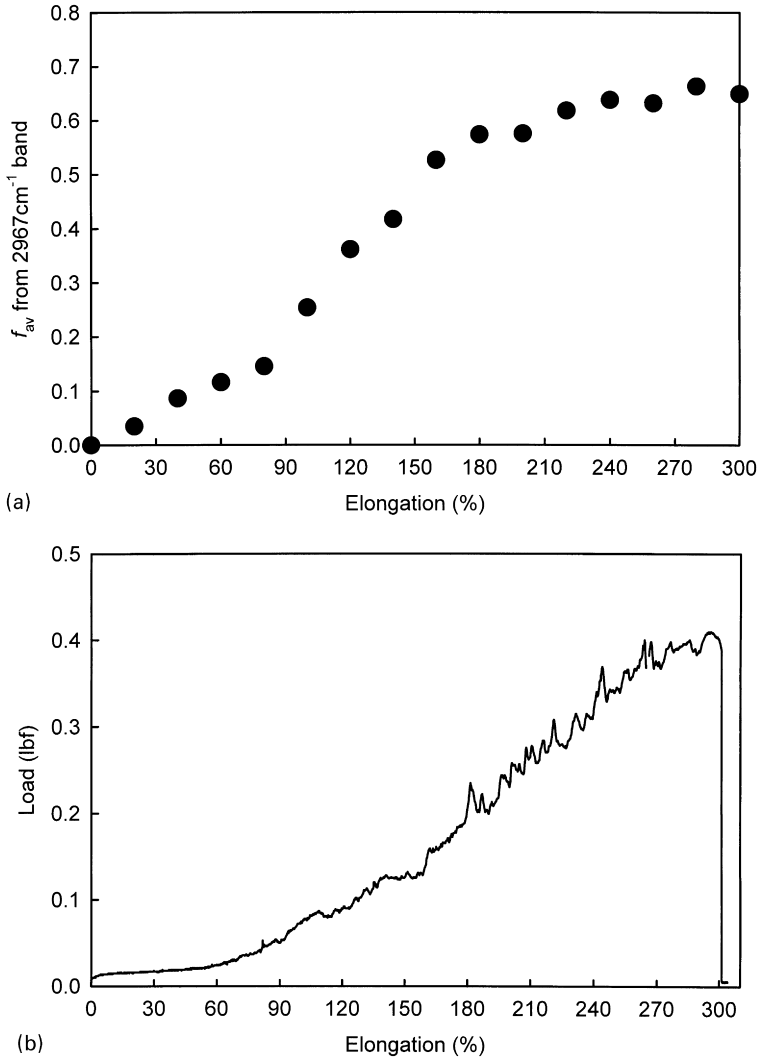

Fig. 9. (a) The variation of the average orientation function calculated from 2967 cm^{-1} upon uniaxial stretching. (b) Load–elongation curve of 3GT film recorded during polarized IR scanning upon drawing.

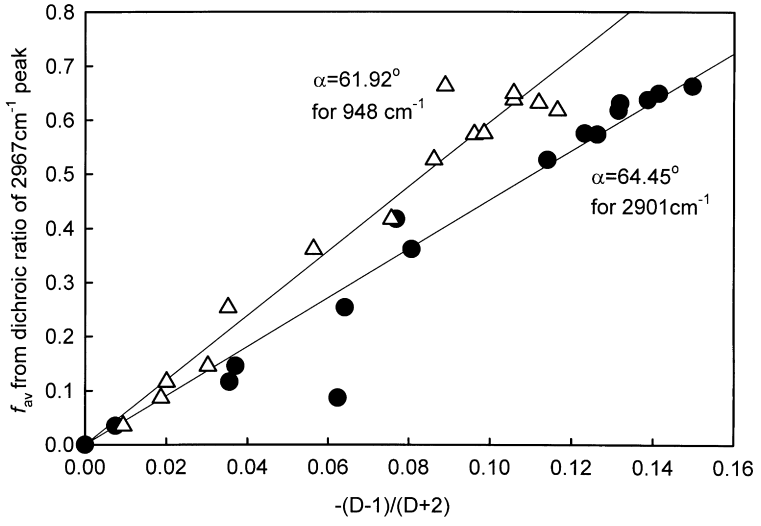

Fig. 10. Determination of the transition moment angle α_v for the 2901 and 948 cm^{-1} bands.

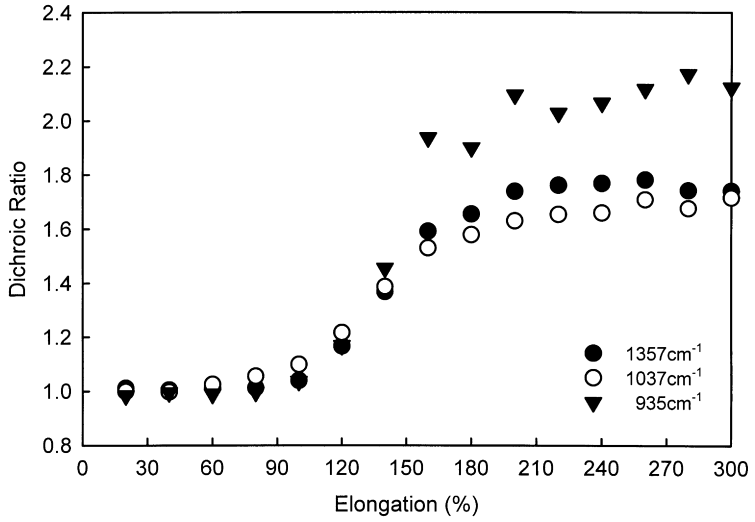

Fig. 11. The variation of the dichroic ratios of the π-bands upon uniaxial stretching.

respectively. Their results are shown in Fig. 12. These three π-peaks also show good linear correlation throughout the entire range.

3.3. Elastic recovery and conformational change upon cyclic loading–unloading

We measured the load–elongation curves of the four-times drawn 3GT film in six cycles of loading–unloading by varying the extension limits from 5 to 20% to find the maximum extension limit within which a compete elastic recovery is observed. These results are depicted in Fig. 13. A complete elastic recovery without a hysteresis loop is seen up to the 10% elongation limit. Above this limit, the hysteresis loop begins to appear. In addition to the appearance of the hysteresis loop, the sample cannot return to its original position because of a kind of permanent set after removing the load, and the remnant elongation increases with the increasing cycles from 13% of maximum elongation. With 20% maximum elongation, very large hysteresis loops are observed and remnant elongation reaches 7–8% after the sixth cycle.

We investigated changes in absorbance with the cyclic extension in several IR spectral regions known to be very sensitive to conformational changes to find the origin of 3GT good elastic recovery. In order to reveal crystal–crystal transition like the reversible $\alpha \rightarrow \beta$ crystal transitions shown by 4GT, several conformationally sensitive regions were investigated. These regions are concerned with C–H bending or methylene rocking modes which exhibit great spectral changes by conformational changes. In these 900–750, 1000–900, and 1495–1345 cm^{-1} spectral regions, 4GT showed great changes in the absorbance of the peaks by the cyclic extension [4]. However, in the case of 3GT, although the position of each characteristic peak is somewhat different with that of 4GT, there were no significant spectral

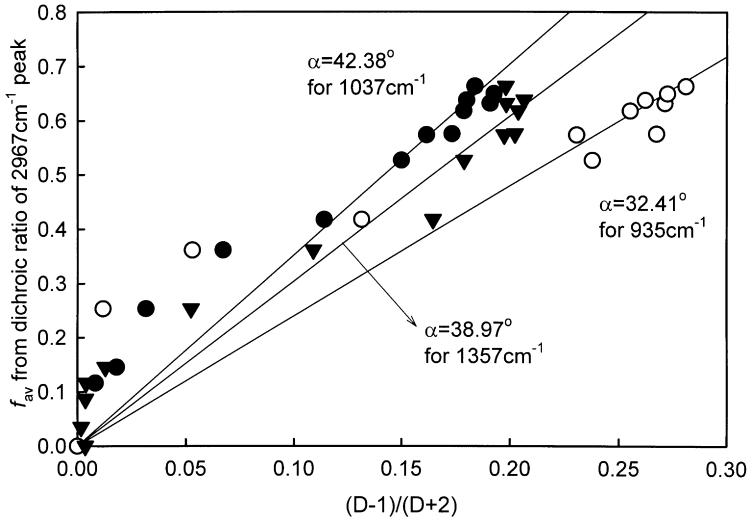

Fig. 12. Determination of the transition moment angle α_v for the 1357, 1037 and 935 cm^{-1} bands.

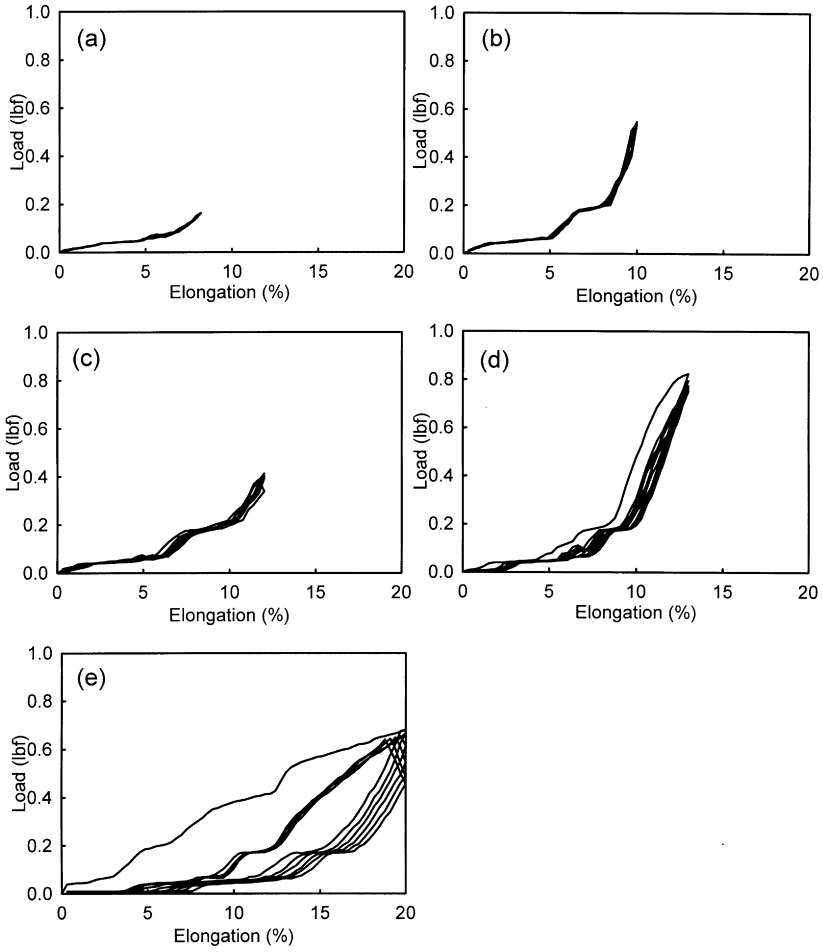

Fig. 13. Elastic recovery of 3GT during 6 cycles of loading–unloading. (a) Maximum elongation = 8%; (b) maximum elongation = 10%; (c) maximum elongation = 12%; (d) maximum elongation = 13%; (e) maximum elongation = 20%.

changes during cyclic extension. This means that there were no changes in the molecular conformation of crystalline regions while the strain was applied and removed periodically. Instead the unit length of the crystal lattice of 3GT was extended by the rotation of C–C–C bond along the axis direction by the applied strain and it came back to the initial value after the removal of the external strain, provided that the strain limit is not greater than 10%; i.e. the molecular chain in the crystalline region behaves like a coiled spring as suggested by Ward and coworkers [1]. They reported that the conformation of 3GT in the crystal lattice is helical with successive monomer units lying at approximately 60° to one another about the helix axis. This helical conformation was identified by the presence of the meridional peak at $2\theta = 12°$ in the X-ray diffraction pattern of the 3GT fiber obtained using FeK_α radiation ($\lambda = 1.936$ Å). When the strain is applied to the drawn 3GT, the meridional peak position is shifted to a lower angle with increasing strain and this change is reversible within the small strain range of ca. 4.5%. From these results, they suggested that the crystal lattice responds immediately to the applied stress and deforms as though it were a coiled spring. Hence 3GT has high elasticity.

4. Conclusions

1. Pure crystalline and amorphous spectra of 3GT can be extracted with factor analysis of IR spectra of 3GT films annealed under various conditions.
2. The fraction of crystalline phase obtained from least-squares curve-fitting in conjunction with factor analysis for an annealed sample showed a very good correlation to the crystallinity obtained by density measurement.
3. The average value of $\cot^2 \alpha_{C=O}$ was calculated to be 0.0738 and $D_{0,C=O}$ was 0.1476 from the crystal lattice parameters of 3GT and the fractional coordinates of each atom in the unit cell.
4. Intrinsic transition moment angles of asymmetric and symmetric stretching vibrations of CH_2, several CH_2 rocking bands, and the 1037 cm^{-1} band could be obtained experimentally in conjunction with changes in dichroic ratio of C=O stretching vibration of the 3GT molecular chain as a function of draw ratio.
5. The analysis of changes in the IR spectrum of 3GT under cyclic loading and unloading revealed no crystal–crystal transitions.

References

[1] Jakeways R, Ward IM, Wilding MA, Hall IH, Desborough IJ, Pass MG. J Polym Sci, Polym Phys Ed 1975;13:799.
[2] Ward IM, Wilding MA, Brody H. J Polym Sci, Polym Phys Ed 1976;14:263.
[3] Miyake A. J Polym Sci 1959;38:479.
[4] Gillette PC, Lando JB, Koenig JL. Polymer 1985;26:235.
[5] Shurvell HF, Bulmer JT. Nomenclature. In: During JR, editor. Vibrational spectra and structure. Amsterdam: Elsevier, 1977 (chap. 2).
[6] Hugus JrZZ, El-Awady AA. J Phys Chem 1971;75:2954.
[7] Bulmer JT, Shurvell HF. J Phys Chem 1973;27:256.
[8] Antoon MK, D'Esposito L, Koenig JL. Appl Spectrosc 1979;33:351.
[9] Koenig JL, Tovar Rodriquez MJM. Appl Spectrosc 1981;35:543.
[10] Knorr FJ, Futrell JH. Anal Chem 1971;51:1236.
[11] Gillette PC, Lando JB, Koenig JL. Anal Chem 1983;55:630.
[12] Culler SR, Gillette PC, Ishida H, Koenig JL. Appl Spectrosc 1984;38:495.
[13] Malinowski ER. Anal Chem 1977;49:606.
[14] Malinowski ER. Anal Chem 1977;49:612.
[15] Malinowski ER, Howery DC. Factor analysis in chemistry. New York: Wiley, 1980.
[16] Kim KJ, Bae JH. J Kor Fib Soc 1996;33:1058.
[17] Stokr J, Schnieder B, Doskocilova D, Lovy J, Sedlacek P. Polymer 1982;23:714.
[18] Dandurand SP, Perez S, Revol JF, Brisse F. Polymer 1979;20:419.
[19] Kim JS, Lewin M, Bulkin BJ. J Polym Sci, Polym Phys Ed 1986;24:1783.
[20] Ward IM, Wilding MA. Polymer 1977;18:327.
[21] Haaland DM, Eastering RG. Appl Spectrosc 1982;36:665.
[22] Samuels RJ. Structured polymer properties. New York: Wiley, 1973 (p. 63–82).
[23] Siesler HW. Advances in polymer science, vol. 65. Heidelberg: Springer, 1985 (p. 9–14).
[24] Fraser RDB. J Chem Phys 1956;24:89.
[25] Hermans JJ, Hermans PH, Vermaas D, Weidinger A. Rec Trav Chim 1946;65:427.
[26] Desborough IJ, Hall IH, Neizzer JZ. Polymer 1979;20:545.